

The Effect of Metal Substitution on the Adsorption Capacity of C24 Fullerene for the Adsorption of Metformin

Mahsa Gooklani*

M.Sc., Chemical Engineering University of Science and Technology of Mazandaran, Babol, Iran

*Corresponding Author Email: mahsagooklani71@gmail.com

Abstract: Metformin is widely used as an antihyperglycemic drug in the treatment of type 2 diabetes and metabolic disorders. Despite its medical benefits, metformin may cause side effects such as hypoglycemia, gastrointestinal disturbances, fatigue, and muscle pain. The development of efficient drug carriers with high adsorption capacity is therefore of great interest. Fullerenes, as a unique class of carbon nanostructures, have attracted attention due to their exceptional electronic and surface properties. In this study, density functional theory (DFT) calculations were performed to investigate the adsorption behavior of metformin on pristine C24 fullerene and metal-substituted fullerenes (Fe, Sc, Zn). Geometry optimizations were carried out using the B3LYP and WB97XD functionals with 3-21G and 6-31G basis sets in the Gaussian software package. Adsorption energies were found to vary depending on the molecular orientation of metformin and the type of metal dopant. Among the systems studied, the Sc-substituted fullerene (C23Sc) exhibited the highest adsorption energy, indicating its potential as an efficient drug carrier. The results demonstrate that metal doping can significantly improve the adsorption performance of C24 for metformin and may contribute to the development of advanced nanocarriers for drug delivery applications.

Keywords: Metformin, fullerene, adsorption energy, density functional theory, drug delivery, metal substitution

Introduction

Metformin (N,N-dimethylimidodicarbonimidic diamide) is one of the most widely prescribed oral antihyperglycemic drugs for the management of type 2 diabetes mellitus (T2DM). As the global prevalence of diabetes continues to increase, the use of metformin has expanded not only due to its glucose-lowering action but also for additional therapeutic roles including weight management, improvement of insulin sensitivity, and treatment of polycystic ovary syndrome (PCOS). Metformin's long clinical history and safety profile make it a first-line therapy in most international guidelines (Esrafil & Khan, 2022). Despite its widespread use, metformin is known to produce gastrointestinal disturbances such as diarrhea, nausea, vomiting, abdominal discomfort, and increased intestinal gas. These side effects significantly affect patient adherence, which is a crucial determinant of glycemic control outcomes. Controlled drug-delivery systems capable of modulating release kinetics and reducing systemic side effects are therefore of considerable interest.

Nanomaterials have emerged as promising candidates for drug encapsulation, adsorption, and controlled release. Among these, carbon-based nanostructures have attracted extraordinary attention due to their unique physicochemical and electronic characteristics. Fullerenes—hollow, cage-like carbon molecules—represent the third

major allotrope of carbon after graphite and diamond. Their discovery opened new domains in nanoscience, leading to substantial applications in photovoltaics, catalysis, sensors, and more recently, nanomedicine. Fullerenes possess high surface curvature, conjugated π -electron networks, and strong electron affinity, enabling efficient interaction with biomolecules. These features make them ideal for exploring new drug-delivery strategies based on adsorption and controlled release (Sadeghzadeh, Sheikhsaie, & Behpour, 2018).

Fullerenes of different sizes and symmetries (C60, C70, C78, C24, etc.) have distinct electronic and geometric characteristics. Smaller fullerenes such as C24, with their higher curvature and reactivity, can exhibit stronger binding with organic molecules compared to larger fullerenes. Their smaller size also makes them promising building blocks for nanoscale biomedical devices due to easier functionalization and enhanced mobility within biological systems (Fekri et al., 2024). However, pristine fullerenes may sometimes display limited interaction with polar drug molecules due to their hydrophobic nature and low inherent dipole moments. Modifying the fullerene structure through heteroatom doping has been shown to significantly enhance their reactivity, charge distribution, and adsorption properties.

Metal substitution—replacing one or more carbon atoms in the fullerene cage with metal atoms—has emerged as a particularly powerful strategy to improve adsorption characteristics. Transition metals such as Fe, Zn, and Sc introduce new electronic states, alter the charge density of the cage, and create localized regions with increased binding affinity for adsorbates. Doping can increase the reactivity by modifying the HOMO–LUMO gap, enhancing charge transfer capability, and introducing favorable coordination sites for polar functional groups. These improvements can be essential for drug-delivery applications involving polar, hydrogen-bonding drugs such as metformin. Therefore, exploring the adsorption behavior of metformin on metal-doped fullerenes has significant value for advancing next-generation nanocarrier design.

Computational chemistry, particularly density functional theory (DFT), has become a cornerstone for evaluating interactions at the molecular and electronic levels. DFT enables accurate modelling of optimized geometries, charge transfer, adsorption energies, molecular orbitals, and interaction mechanisms in complex systems. The foundation of DFT lies in the Hohenberg–Kohn theorems, which state that the ground-state energy of a many-electron system is uniquely determined by its electron density. This concept allows computational chemists to treat interacting electrons through universal energy functionals, achieving a balance between computational efficiency and accuracy. For adsorption studies on nanostructures, DFT provides detailed insight into binding mechanisms, stability, and electronic properties, making it an indispensable tool for designing nanocarrier systems without the need for initial experimental trials (Iskender Muz, 2025).

The present study focuses on modeling the adsorption behavior of metformin on pristine C24 fullerene and its metal-substituted variants: C23Fe, C23Zn, and C23Sc. The choice of metals is motivated by their distinct electronic structures and functional significance. Iron, a transition metal with high catalytic activity, can significantly influence the electronic reactivity of carbon frameworks. Zinc, a commonly used dopant with moderate electronegativity, can modify local charge distribution while maintaining structural stability. Scandium, a transition metal with large ionic radius and low electronegativity, is known to strongly distort fullerene cages and dramatically enhance adsorption tendencies.

Using DFT calculations with B3LYP and WB97XD functionals and 3-21G and 6-31G basis sets, this study evaluates how metal substitution affects adsorption energies, geometric configuration, and electronic properties of metformin–fullerene complexes. Understanding the variation in adsorption effects provides deeper insight into the mechanistic role of metal dopants in enhancing drug–carrier interactions. This research not only delivers key theoretical foundations for the use of metal-doped fullerenes as potential nanocarriers but also guides future experimental efforts in synthesizing functionalized fullerene-based delivery systems with tunable binding affinity and controlled drug release characteristics.

Methodology

Molecular Structure Simulation Approaches

Molecular systems can be simulated using either classical or quantum-based computational methods. Classical techniques, such as Monte Carlo simulations and molecular dynamics, are widely used to study equilibrium and non-equilibrium processes. However, these approaches are limited in their ability to accurately describe adsorption mechanisms at the atomic scale, particularly when electronic interactions play a significant role. For adsorption studies requiring detailed interpretation of electronic behavior, quantum-mechanical methods—either semi-empirical or ab initio—offer a more reliable and realistic description.

Computational Framework

In quantum chemical modeling, two central components are required:

1. **A calculation method**, such as molecular mechanics, semi-empirical approaches, or density functional theory (DFT).
2. **An approximation method**, such as Hartree–Fock or related techniques.

Advances in computational power have enabled researchers to model increasingly large and complex molecular systems. After defining the molecule of interest, geometry optimization is performed to identify the minimum-energy structure, which then serves as the basis for calculating the molecule's physical and chemical properties.

Gaussian Software

All quantum chemical calculations in this study were conducted using the Gaussian software package. Gaussian was originally introduced by John Pople in 1987 and has undergone multiple developmental iterations, including Gaussian 76, 80, 82, 94, 98, 03, and the currently used Gaussian 09. Gaussian enables users to select an appropriate level of theory and basis set based on the goals and complexity of the system.

For the investigation of metformin adsorption on the C₂₄ fullerene, two types of calculations were performed:

1. **Geometry optimization**
2. **Total energy calculations**

Gaussian, written in Fortran, supports a wide range of computational tasks, including geometry optimization, vibrational frequency analysis, transition-state structure determination, thermochemical calculations, bond energies, reaction pathways, molecular orbital analysis, atomic charge distribution, multipole moments, electron affinity, and electron density mapping. These analyses can be applied to molecules in the gas phase or in solution and in either the ground or excited state.

Density Functional Theory Calculations

DFT was employed for both geometry optimization and electronic structure analysis. Frontier molecular orbital energies (HOMO and LUMO) were calculated using the NBO module within Gaussian. Optimizations were performed using the **3-21G basis set**, suitable for first-row elements. For systems requiring higher precision, reference was made to the **6-31G** basis set, commonly used for third-row atoms.

B3LYP Functional

The **B3LYP** hybrid functional was selected to evaluate geometric parameters, atomic charges, and bond characteristics. B3LYP provides reliable activation energies and enthalpies while maintaining computational efficiency, even with relatively small basis sets. This functional is known for low root-mean-square errors and good equilibrium structure prediction, making it suitable for reaction energy and adsorption studies.

Overview of Basis Sets

In quantum chemistry, a **basis set** is a collection of mathematical functions used to construct molecular orbitals. These functions, typically centered on atomic nuclei, approximate the true atomic orbitals and allow the electronic structure of a molecule to be calculated. Molecular orbitals are expressed as linear combinations of basis functions, with coefficients determined through quantum mechanical computations.

Larger basis sets provide more accurate representations of electron distribution and can better account for electron correlation and spatial flexibility. However, they require greater computational cost and additional approximations. Even for simple atoms such as hydrogen, basis functions remain approximations to the true wavefunctions.

Categories of Basis Sets

Basis sets are generally divided into two main groups:

1. **Simple (or standard) basis sets**
2. **Extended (or advanced) basis sets**

The simple basis sets commonly used in electronic-structure calculations include:

Minimal Basis Sets

A minimal basis set assigns **one basis function to each atomic orbital**. These functions have fixed shapes and represent only the occupied atomic orbitals of the atom. Minimal basis sets are often denoted as **STO-nG**, where *n*

indicates the number of primitive Gaussian functions combined to approximate a Slater-type orbital. For example, STO-3G uses three Gaussian primitives for each basis function.

Split-Valence Basis Sets

Split-valence basis sets expand upon minimal sets by using **multiple functions to represent valence orbitals**, which participate most directly in chemical bonding. Inner-shell orbitals are typically represented by a single function, while valence orbitals are split into two or more functions to improve flexibility. Common split-valence sets include **3-21G** and **6-31G**, which assign two or more functions per valence orbital.

Polarization Functions

Although split-valence sets allow orbital size to vary, they do not allow changes in orbital shape. **Polarization functions** introduce orbitals with higher angular momentum (e.g., adding d-functions to carbon or p-functions to hydrogen). These functions enable molecular orbitals to deform appropriately during bonding and reactivity. Polarized basis sets are often indicated by an asterisk, *such as 6-31G*.

Diffuse Functions

Diffuse functions are additional Gaussian functions with very small exponents, added to describe the **outer regions of electron density**, particularly important for anions, Rydberg states, weak interactions, and large or loosely bound systems. They are denoted by + or ++ signs (e.g., **6-31+G** or **6-31++G**), where the double plus indicates diffuse functions added to both heavy atoms and hydrogens.

Energy Determination Methods

B3LYP Functional: The B3LYP method combines Becke's three-parameter hybrid exchange functional (B3) with the correlation functional developed by Lee, Yang, and Parr (LYP). The LYP functional accounts for electron correlation through an approximate gradient-corrected (GGA) formulation. When combined, the B3 and LYP components form the **B3LYP hybrid functional**, one of the most widely used and reliable density functional theory (DFT) approaches. Numerous computational studies have demonstrated that B3LYP provides accurate and consistent results across a broad range of molecular systems, making it a robust method for calculating correlation energies, molecular structures, and thermodynamic properties.

WB97XD Functional: The WB97XD functional, developed by Head-Gordon and co-workers, is a long-range corrected hybrid functional enhanced with empirical dispersion (D) corrections. It incorporates variable exchange contributions and improved treatment of non-covalent interactions. WB97XD is considered one of the most accurate and efficient modern DFT functionals, particularly for systems where dispersion interactions or long-range electronic effects are significant. In many cases, WB97XD exhibits lower error than earlier hybrid functionals such as B3LYP.

Quantum Mechanical Methods

Quantum mechanical calculations determine molecular energies and properties by solving the Schrödinger equation (SE). The SE fully defines the molecular wavefunction; however, exact analytical solutions are only possible for simple one-electron systems like the hydrogen atom. For all multi-electron systems, approximate methods are required to obtain practical solutions.

Hartree–Fock Approximation

The Hartree–Fock (HF) method is one of the foundational approximations used to solve the Schrödinger equation for many-electron systems. In this approach, molecular orbitals are expressed as linear combinations of predefined basis functions. Because the HF equations depend on the orbitals they seek to determine, they are solved iteratively using the **self-consistent field (SCF)** method.

Exact HF results are only approached when an infinitely large basis set is used—an impossibility in practice. Therefore, finite and truncated basis sets are employed, yielding approximate but often highly useful solutions. The accuracy of the HF method depends significantly on the quality and design of the chosen basis set.

Density Functional Theory (DFT)

DFT has emerged as one of the most powerful and widely used methods for computing electron correlation effects. Initially developed for solid-state physics, DFT evaluates exchange-correlation energies as functions of electron density rather than explicit many-electron wavefunctions.

DFT is grounded in the **Hohenberg–Kohn theorems**, which establish that (1) the ground-state electron density uniquely determines all electronic properties of a system, and (2) the ground-state energy can be obtained using a suitable energy functional of the density. Consequently, DFT replaces complex many-electron wavefunctions with the electron density as the central quantity.

DFT methods offer several advantages:

- Good agreement with experimental results for many solid-state and molecular systems
- Significantly lower computational cost compared to multi-electron wavefunction-based methods (e.g., HF, post-HF methods)
- Efficient calculation of ground-state energies, optimized geometries, and electronic properties

However, a key challenge remains: the exact exchange-correlation functional is unknown, and practical DFT relies on approximate functionals such as LYP, B3LYP, or WB97XD. Additionally, although DFT calculations yield orbitals, these orbitals lack a direct physical interpretation compared to Hartree–Fock orbitals.

Modeling Procedure

Molecular modeling constituted a central component of this study, as the accuracy of the modeled structures directly influences the reliability and computational efficiency of subsequent calculations. All molecular structures—including metformin, pristine fullerene, and metal-doped fullerenes—were first constructed and then fully optimized using quantum chemical methods.

Fullerenes were doped with Fe, Sc, and Zn atoms, and each doped structure was optimized prior to adsorption modeling. To generate realistic adsorption configurations, the metal centers were systematically positioned near metformin from multiple orientations, and preliminary optimizations were performed to identify the most probable initial geometries. These optimized configurations were then used as starting points for evaluating the interaction between metformin and the doped fullerenes.

After establishing appropriate adsorption sites on the fullerene surface, final geometry optimizations were conducted for all metformin–fullerene complexes. Adsorption energies were calculated using density functional theory (DFT), employing both the **B3LYP** and **WB97XD** functionals. Thermodynamic quantities—including enthalpy, entropy, Gibbs free energy, and charge distribution—were also computed to assess the stability and determine the most energetically favorable adsorption configuration.

The overall modeling workflow ensured accurate structural prediction, efficient convergence, and reliable evaluation of adsorption properties across all metal-doped fullerene systems studied.

Optimization

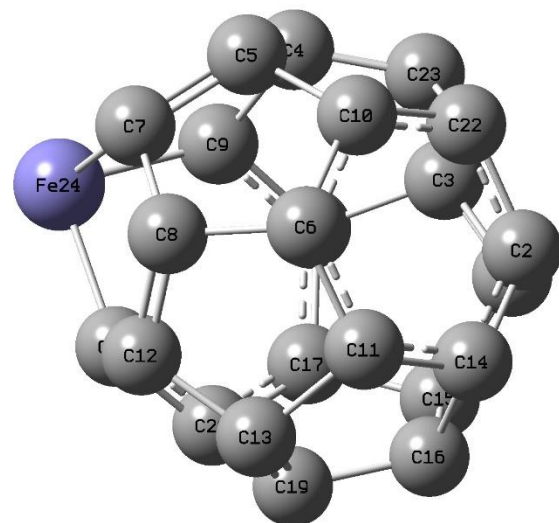


Figure 1. C23Fe after optimization

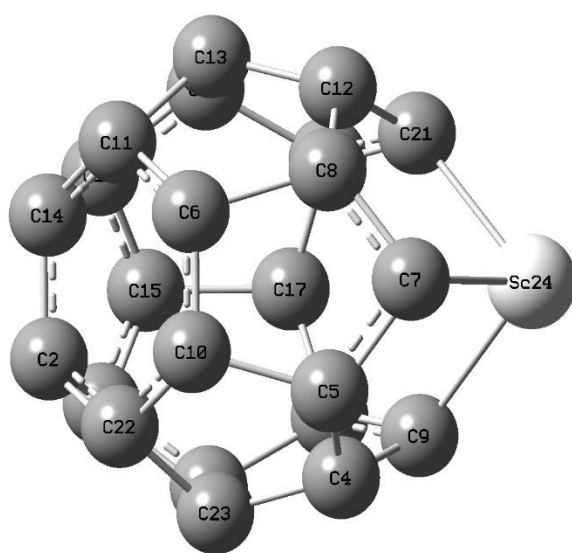


Figure 2. C₂₃Sc after optimization

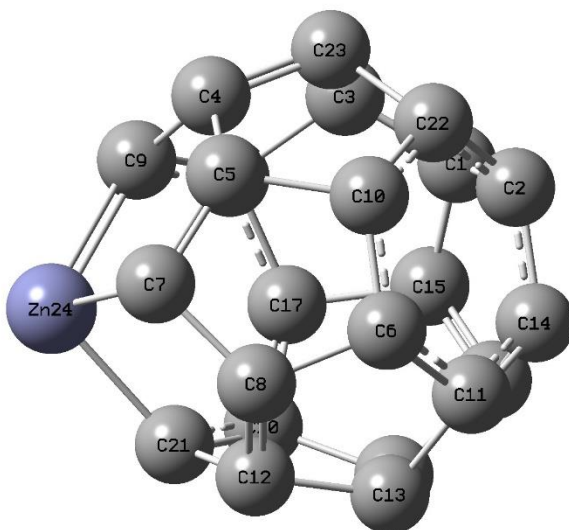


Figure 3. C₂₃Zn after optimization

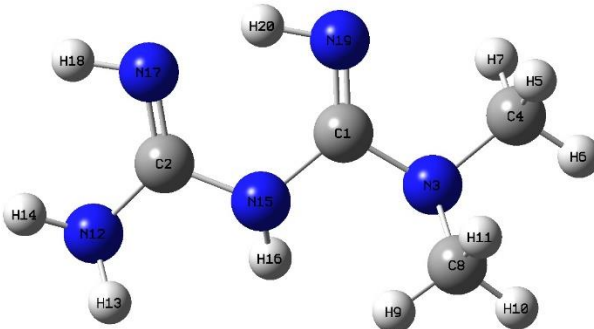


Figure 4. Metformin drug after optimization

Adsorption Energy Calculation

The adsorption energy ($E_{\text{adsorbate}}$) for each metformin–fullerene complex was calculated using:

$$E_{\text{adsorbate}} = E_{\text{complex}} - (E_{\text{adsorbent}} + E_{\text{drug}}) \quad (3-1)$$

This expression quantifies the interaction strength between metformin and the metal-doped fullerene adsorbent.

Thermodynamic Parameters

Thermodynamic quantities—including Gibbs free energy (ΔG), enthalpy (ΔH), and entropy (ΔS)—were obtained using the following relations:

$$\Delta G = G_{\text{complex}} - (G_{\text{drug}} + G_{\text{adsorbent}}) \quad (3-2)$$

$$\Delta H = H_{\text{complex}} - (H_{\text{adsorbent}} + H_{\text{drug}}) \quad (3-3)$$

$$\Delta S = \frac{\Delta H - \Delta G}{T} \quad (3-4)$$

Here:

- E_{ads} , G_{ads} , H_{ads} , S_{ads} correspond to the energy, Gibbs free energy, enthalpy, and entropy of each metal-doped adsorbent.
- E_{drug} , G_{drug} , H_{drug} , S_{drug} represent the corresponding thermodynamic quantities of metformin.
- E_{complex} , G_{complex} , H_{complex} , S_{complex} represent the values for the metformin–fullerene complex.

Frontier Molecular Orbital (FMO) Analysis

The electronic properties of all structures were evaluated through frontier molecular orbital calculations. The HOMO–LUMO energy gap (E_g) is defined as:

$$E_g = E_{\text{LUMO}} - E_{\text{HOMO}}$$

A smaller energy gap indicates increased molecular polarization and higher electronic conductivity, whereas a larger gap corresponds to higher chemical stability and reduced reactivity of the drug–adsorbent system.

The HOMO (highest occupied molecular orbital) contains the highest-energy electrons available for interaction, while the LUMO (lowest unoccupied molecular orbital) represents the lowest-energy orbital capable of accepting an electron. The HOMO–LUMO gap therefore reflects the minimum excitation energy required for electronic transitions within the molecule.

Charge Analysis

Charge analysis was performed to evaluate electron distribution, intramolecular interactions, and charge transfer within the studied molecules. **Natural Bond Orbital (NBO) analysis** was employed to investigate particle interactions and quantify electron delocalization. A key advantage of NBO analysis is its adaptability to structural changes, accommodating both radial and angular variations in the molecular geometry, making it particularly suitable for studying adsorption complexes and metal–ligand interactions.

Results

Structural Optimization of the C24 Fullerene

To determine the most stable structure of the C24 fullerene, geometry optimization was first performed using density functional theory (DFT) with the **B3LYP method and the 3-21G basis set**. In the next step, structural optimization was refined using the **WB97XD method and the 6-31G basis set** to properly account for dispersion interactions and improve the accuracy of adsorption energy calculations.

Adsorption of Metformin on Metal-Doped Fullerene (Fe, Sc, Zn)

Adsorption of Metformin on Fe-Doped Fullerene: The adsorption energies of metformin on Fe-doped fullerene (C23Fe) were computed at the **B3LYP/3-21G** level for five adsorption configurations. The results are summarized in [Table 1](#).

Table 1. Adsorption energies of C23Fe–Metformin (B3LYP/3-21G)

Sample	Adsorption Energy (E _{ad}) (kcal/mol)
C23Fe-M1	-935.41
C23Fe-M2	-468.65
C23Fe-M3	-2799.68
C23Fe-M4	-744.67
C23Fe-M5	-357.49

As shown in [Table 1](#), the M2 and M3 configurations exhibited the most favorable adsorption energies (-468.65 and -2799.68 kcal/mol). These two were further evaluated using a more accurate functional.

The **WB97XD/6-31G** results are presented in [Table 2](#).

Table 2. Adsorption energies of C23Fe–Metformin (WB97XD/6-31G)

Sample	Adsorption Energy (E _{ad}) (kcal/mol)
WC23Fe-M2	-137.38
WC23Fe-M3	-138.09

Since metformin adsorption occurs in a liquid environment, solvent-phase calculations (water) were performed. The results are shown in [Table 3](#).

Table 3. Adsorption energies of C23Fe–Metformin in Solvent Phase (Water)

Sample	Adsorption Energy (E _{ad}) (kcal/mol)
Solvent C23Fe-M2	-158.35
Solvent C23Fe-M3	-136.37

Adsorption of Metformin on Sc-Doped Fullerene

The adsorption energies calculated for six configurations of C23Sc–Metformin using the **B3LYP/3-21G** method are shown in [Table 4](#).

Table 4. Adsorption energies of C23Sc–Metformin (B3LYP/3-21G)

Sample	Adsorption Energy (E _{ad}) (kcal/mol)
C23Sc-M1	-360.37
C23Sc-M2	-739.62
C23Sc-M3	-3621.63

Sample	Adsorption Energy (E _{ad}) (kcal/mol)
C23Sc-M4	-115.65
C23Sc-M5	-532.37
C23Sc-M6	-567.41

The M2 and M3 configurations again showed the strongest adsorption and were subsequently recalculated using the **WB97XD/6-31G** method ([Table 5](#)).

Table 5. Adsorption energies of C23Sc–Metformin (WB97XD/6-31G)

Sample	Adsorption Energy (E _{ad}) (kcal/mol)
WC23Sc-M2	-139.28
WC23Sc-M3	-148.02

To simulate biological and environmental conditions, the adsorption energies were recalculated in the solvent phase (water). Results are listed in [Table 6](#).

Table 6. Adsorption energies of C23Sc–Metformin in Solvent Phase (Water)

Sample	Adsorption Energy (E _{ad}) (kcal/mol)
Solvent C23Sc-M2	-129.27
Solvent C23Sc-M3	-157.37

Adsorption of Metformin on Zn-Doped Fullerene

Adsorption energies of metformin on Zn-doped fullerene (C23Zn) were calculated at the **B3LYP/3-21G** level for six configurations. The results are summarized in [Table 7](#).

Table 7. Adsorption energies of C23Zn–Metformin (B3LYP/3-21G)

Sample	Adsorption Energy (E _{ad}) (kcal/mol)
C23Zn-M1	-434.44
C23Zn-M2	-9986.64
C23Zn-M3	-1116.65
C23Zn-M4	-641.62
C23Zn-M5	-338.43
C23Zn-M6	-587.59

The M2 and M3 configurations were then optimized using the **WB97XD/6-31G** functional. Results are presented in [Table 8](#).

Table 8. Adsorption energies of C23Zn–Metformin (WB97XD/6-31G)

Sample	Adsorption Energy (E _{ad}) (kcal/mol)
WC23Zn-M2	-136.55
WC23Zn-M3	-135.65

Finally, solvent-phase adsorption energies were obtained and are listed in [Table 9](#).

Table 9. Adsorption energies of C23Zn–Metformin in Solvent Phase (Water)

Sample	Adsorption Energy (E _{ad}) (kcal/mol)
Solvent C23Zn-M2	-133.56
Solvent C23Zn-M3	-135.55

Enthalpy Study of Metformin Complexes with C24 Derivatives

To further understand the thermodynamic behavior of metformin adsorption on metal-doped fullerene derivatives, enthalpy (ΔH) values were calculated for the optimized complexes in the solvent phase (water). The results for Fe-, Sc-, and Zn-doped C23 fullerene systems are summarized in [Table 10](#).

Table 10. Enthalpy of Metformin Complexes with Fe-, Sc-, and Zn-Doped C23 Fullerene (Solvent Phase, kcal/mol)

Sample	Enthalpy (ΔH) (kcal/mol)
Solvent C23Fe-M2	-315.59
Solvent C23Fe-M3	-354.42
Solvent C23Sc-M2	-243.64
Solvent C23Sc-M3	-349.06
Solvent C23Zn-M2	-327.48
Solvent C23Zn-M3	-338.80

As shown in Table 10, all complexes exhibit **negative enthalpy values**, indicating that the adsorption of metformin onto the doped fullerene surfaces is **exothermic and thermodynamically favorable** in aqueous solution. Among the studied systems, the Sc-doped complexes—especially **Solvent C23Sc-M3**—show the most negative enthalpy values, suggesting stronger thermodynamic stability compared to the Fe- and Zn-doped systems.

Entropy Study of Metformin Complexes with C24 Derivatives

To complement the enthalpy analysis, entropy (ΔS) values were calculated for the metformin complexes formed with Fe-, Sc-, and Zn-doped C23 fullerene in the solvent phase (water). These entropy values describe the degree of molecular order/disorder upon complex formation and help clarify the thermodynamic behavior of adsorption. The results are summarized in Table 11.

Table 11. Entropy of Metformin Complexes with Fe-, Sc-, and Zn-Doped C23 Fullerene (Solvent Phase, kcal/mol·K)

Sample	Entropy (ΔS) (kcal/mol·K)
Solvent C23Fe-M2	-0.0297
Solvent C23Fe-M3	-0.0408
Solvent C23Sc-M2	-0.0369
Solvent C23Sc-M3	-0.0433
Solvent C23Zn-M2	-0.0443
Solvent C23Zn-M3	-0.0394

As presented in Table 11, all calculated entropy values are negative, indicating a **decrease in molecular disorder upon complex formation**, which is characteristic of adsorption processes where the drug binds to a fixed surface. Among the studied systems, Zn- and Sc-doped fullerenes show slightly more negative entropy changes, suggesting a stronger ordering effect when metformin is adsorbed onto these doped surfaces.

Gibbs Free Energy Study of Metformin Complexes with C24 Derivatives

Gibbs free energy (ΔG) was calculated to evaluate the overall spontaneity of metformin adsorption on Fe-, Sc-, and Zn-doped C23 fullerene structures in the solvent phase (water). Negative ΔG values indicate spontaneous and thermodynamically favorable adsorption. The computed results are summarized in Table 12.

Table 12. Gibbs Free Energy of Metformin Complexes with Fe-, Sc-, and Zn-Doped C23 Fullerene (Solvent Phase, kcal/mol)

Sample	Gibbs Free Energy (ΔG) (kcal/mol)
Solvent C23Fe-M2	-221.64
Solvent C23Fe-M3	-232.84
Solvent C23Sc-M2	-135.73
Solvent C23Sc-M3	-213.68
Solvent C23Zn-M2	-195.55
Solvent C23Zn-M3	-228.05

As shown in Table 12, all ΔG values are **negative**, confirming that adsorption of metformin on Fe-, Sc-, and Zn-doped fullerene is **spontaneous in aqueous solution**. Among the studied systems, Fe-doped and Zn-doped fullerenes—particularly **Solvent C23Fe-M3** and **Solvent C23Zn-M3**—show the most negative Gibbs free energy values, indicating stronger spontaneity and higher stability of the resulting complexes in solution.

Review of HOMO and LUMO orbitals

HOMO and LUMO orbitals of the C₂₃Fe molecule

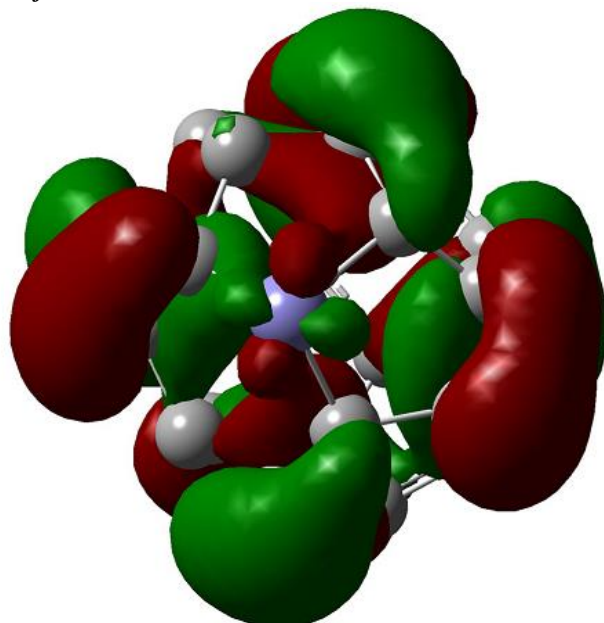


Figure 5. HOMO orbital of Solvent C₂₃Fe

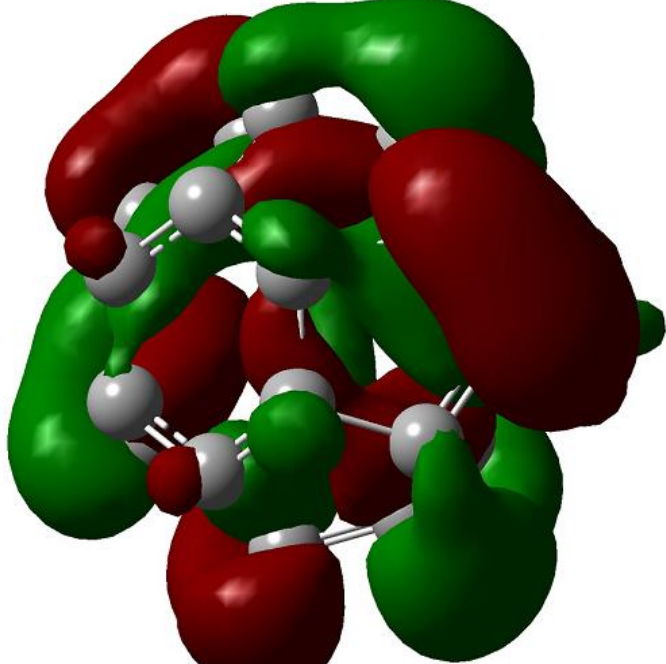


Figure 6. LUMO orbital of Solvent C₂₃Fe

HOMO and LUMO orbitals of the C23Fe molecule and metformin

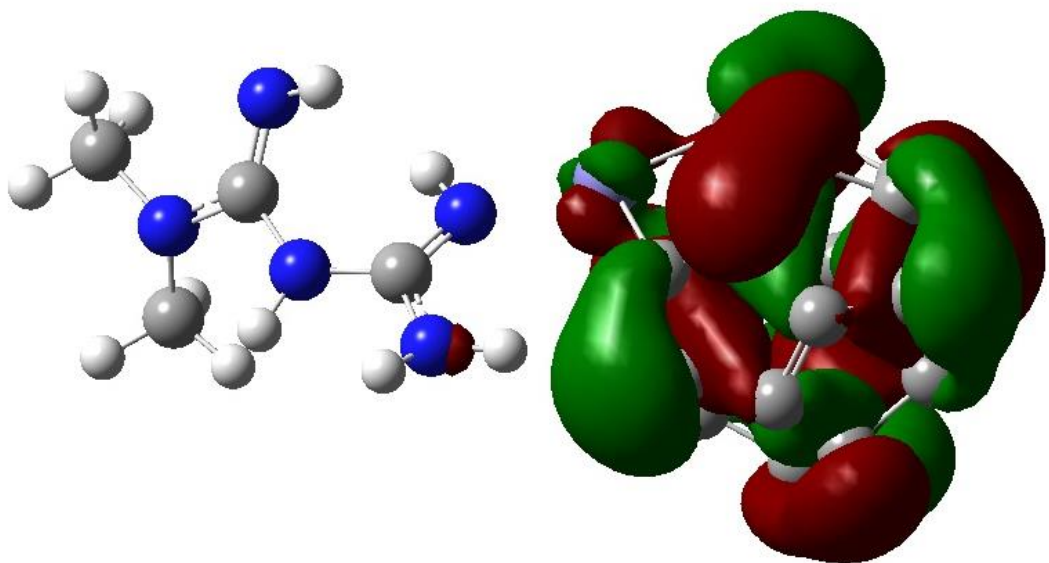


Figure 7. HOMO orbital of Solvent C23FeM2

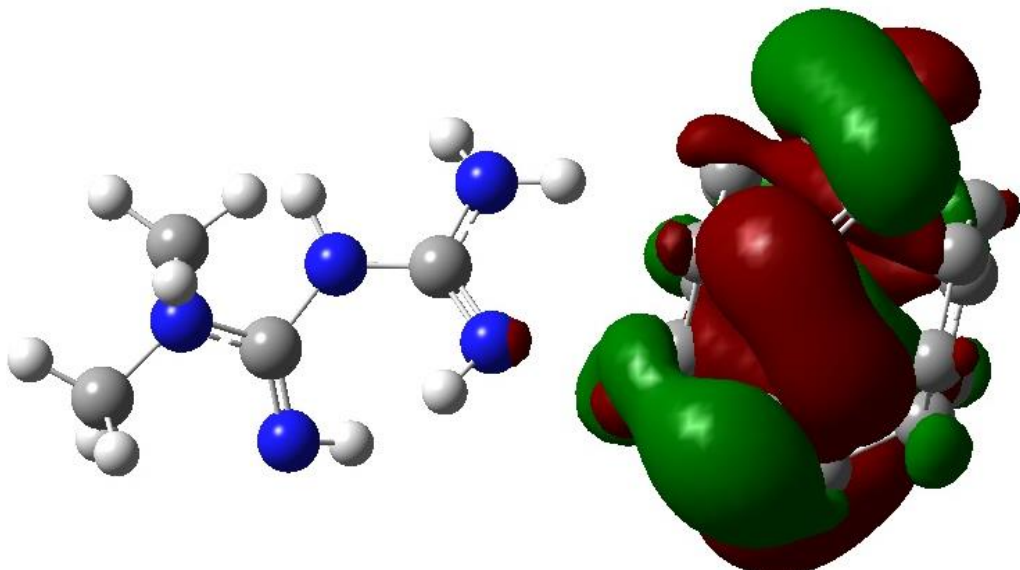


Figure 8. LUMO orbital of Solvent C23Fe M2

HOMO and LUMO orbitals of the C23FeM3 molecule and metformin

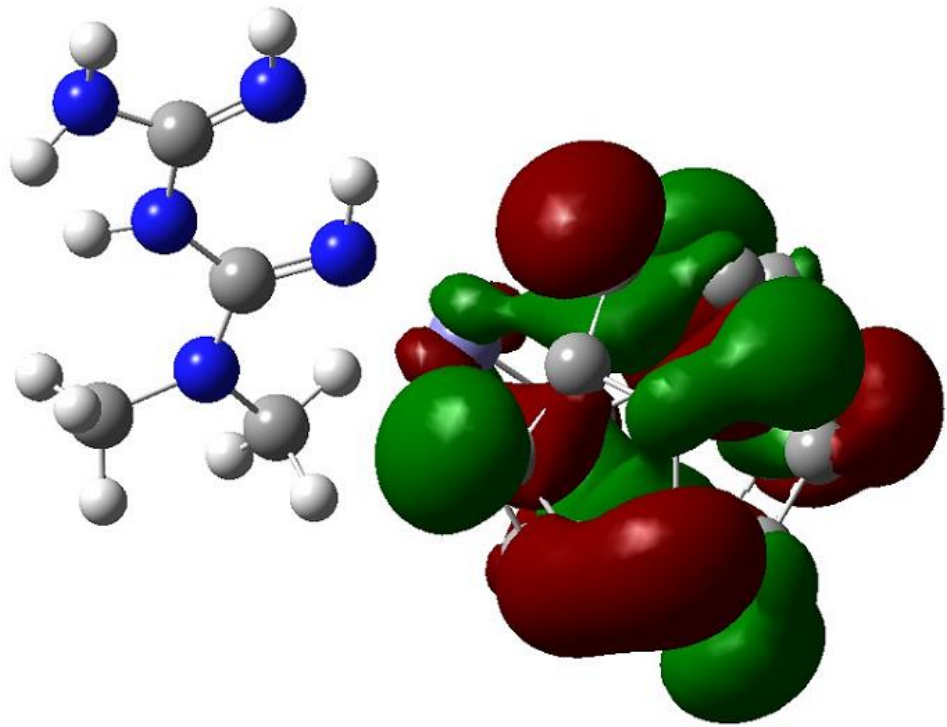


Figure 9. HOMO orbital of Solvent C23Fe M3

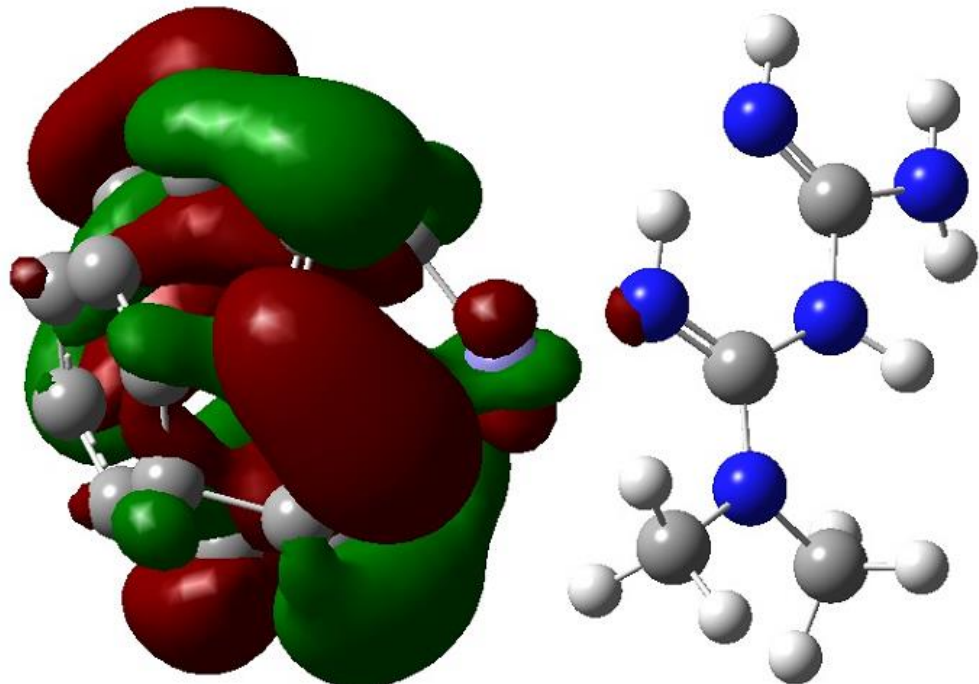


Figure 10. LUMO orbital of Solvent C23Fe M3

HOMO and LUMO orbitals of the C23Sc molecule

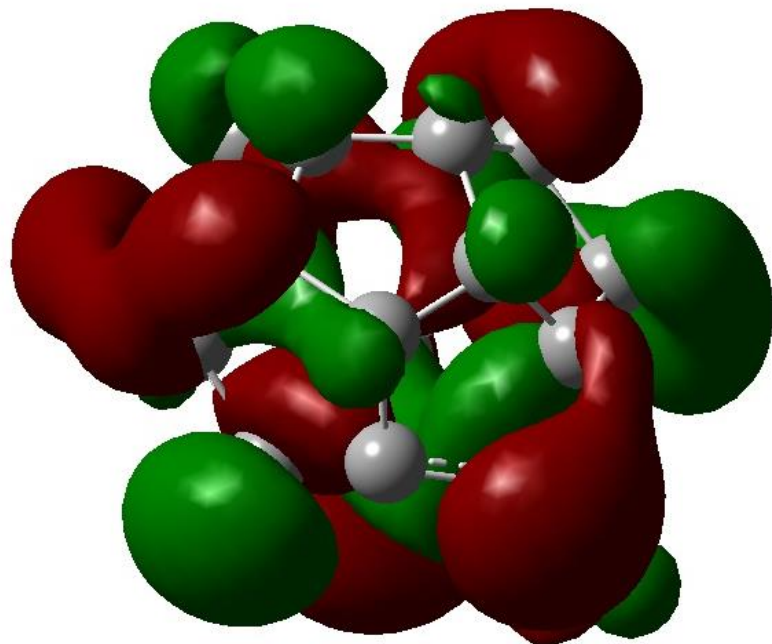


Figure 11. HOMO orbital of Solvent C23Sc

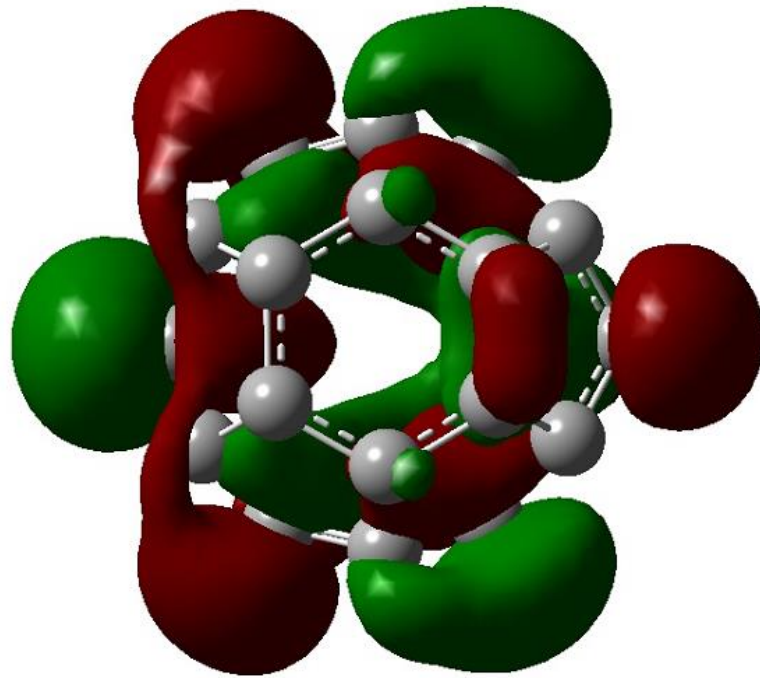


Figure 12. LUMO orbital of Solvent C23Sc

HOMO and LUMO orbitals of the C23Sc molecule and metformin

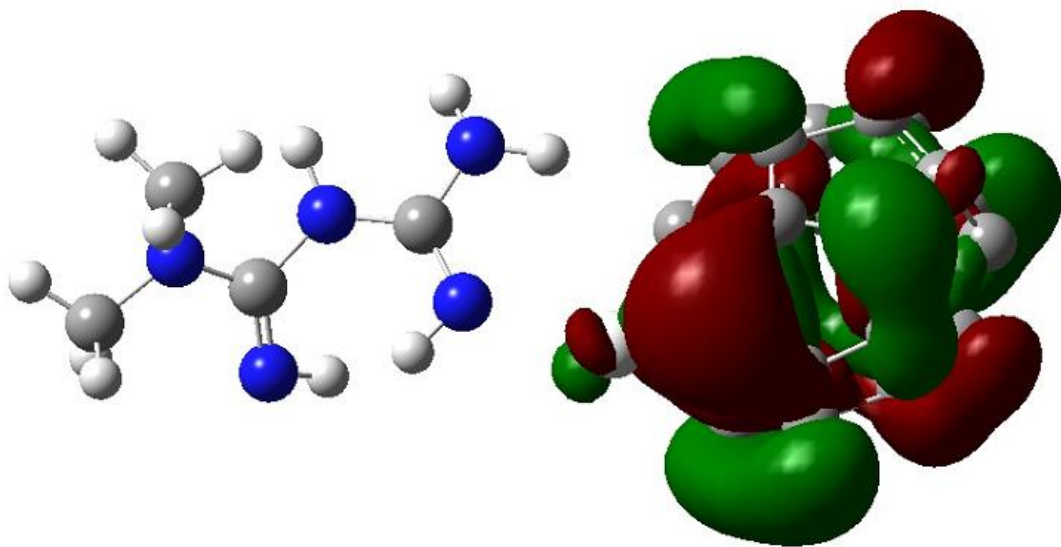


Figure 13. HOMO orbital of Solvent C23Sc M2

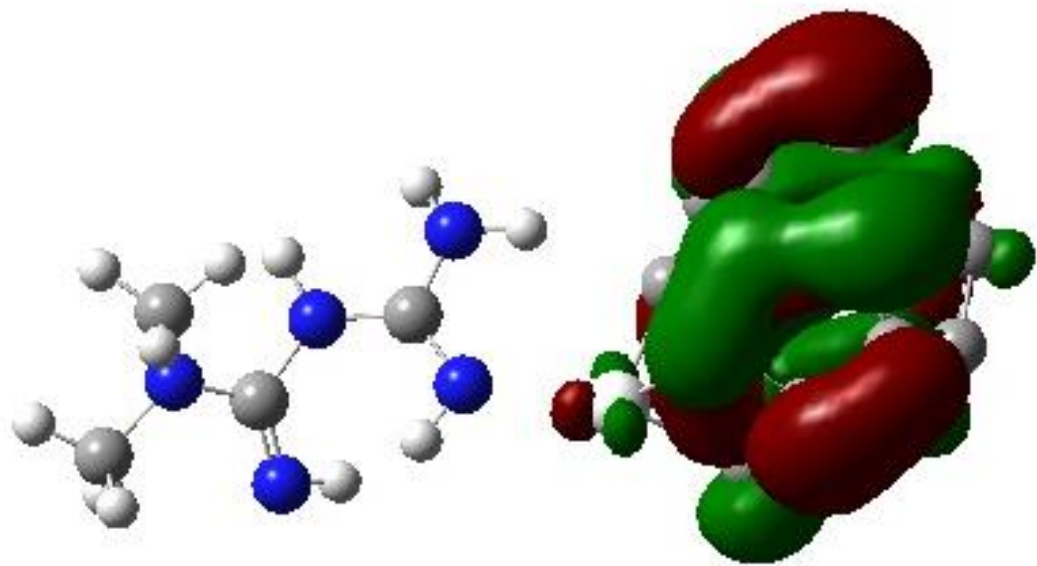


Figure 14. LUMO orbital of Solvent C23Sc M2

HOMO and LUMO orbitals of the C23ScM3 molecule and metformin

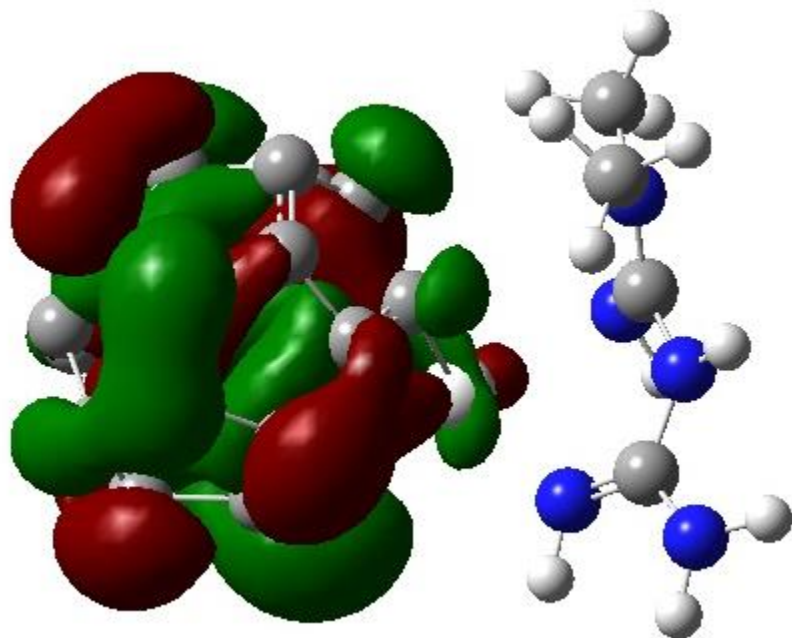


Figure 15. HOMO orbital of Solvent C23Sc M3

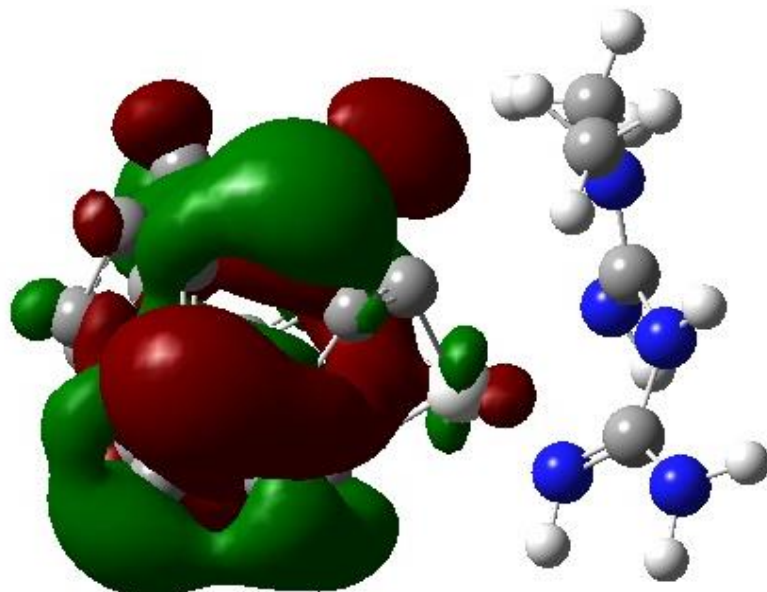


Figure 16. LUMO orbital of Solvent C23ScM3

Orbitals HOMO and LUMO of the C23Zn molecule

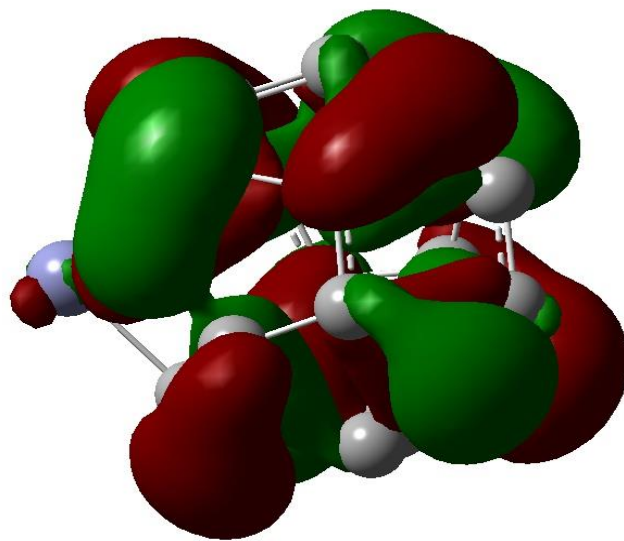


Figure 17. HOMO orbital of Solvent C23Zn

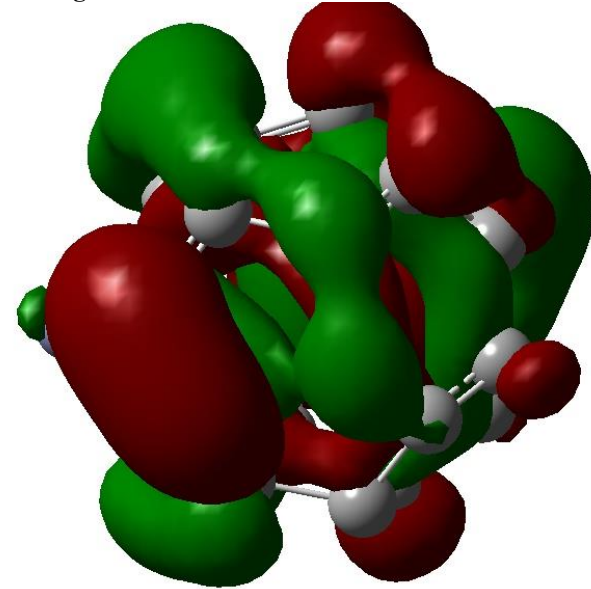


Figure 18. LUMO orbital of Solvent C23Zn

HOMO and LUMO orbitals of the C23Zn molecule and metformin

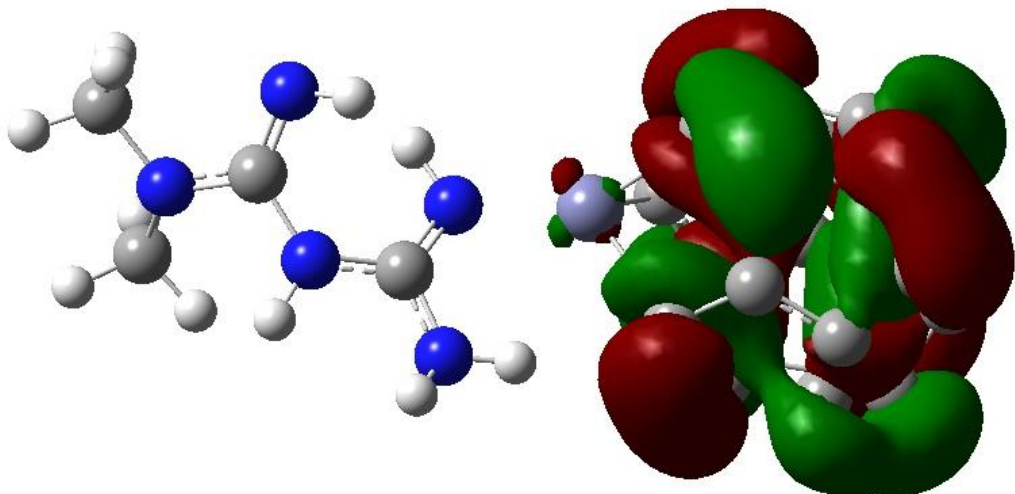


Figure 19. HOMO orbital of Solvent C23Zn M2

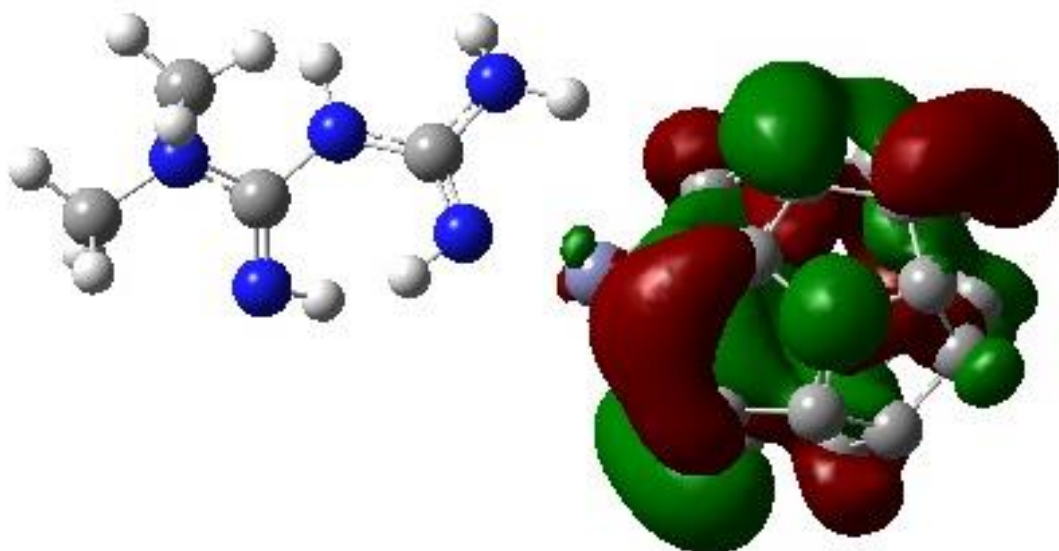


Figure 20. LUMO orbital of Solvent C23Zn M2

HOMO and LUMO orbitals of the C23ZnM3 molecule and metformin

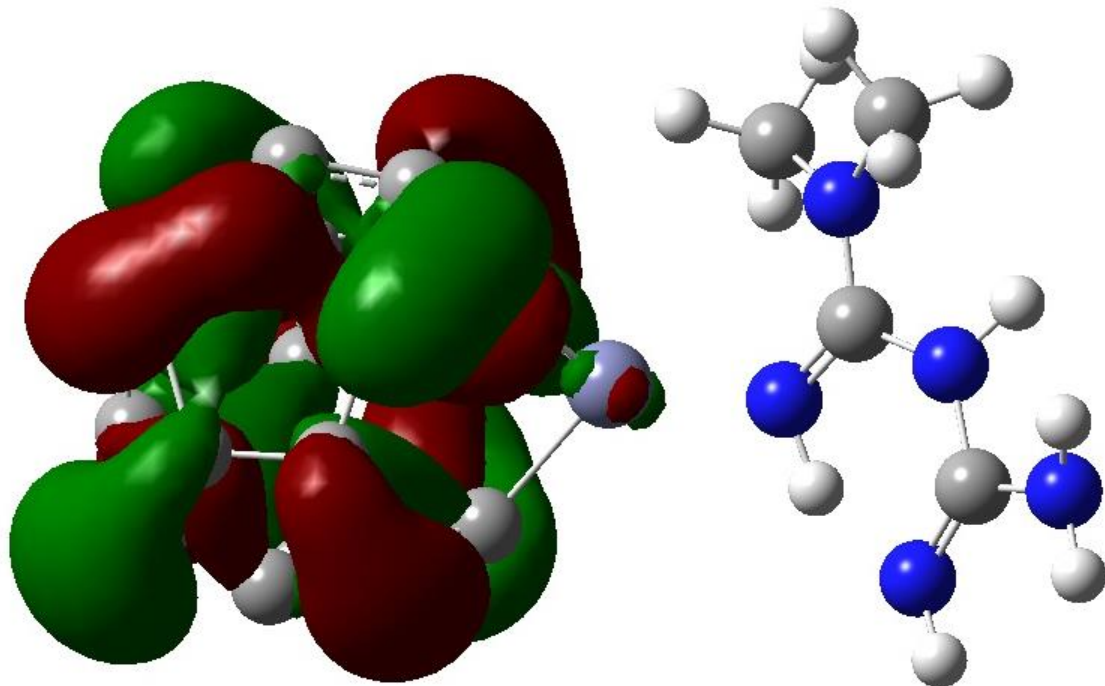


Figure 21. HOMO orbital of Solvent C23Zn M3

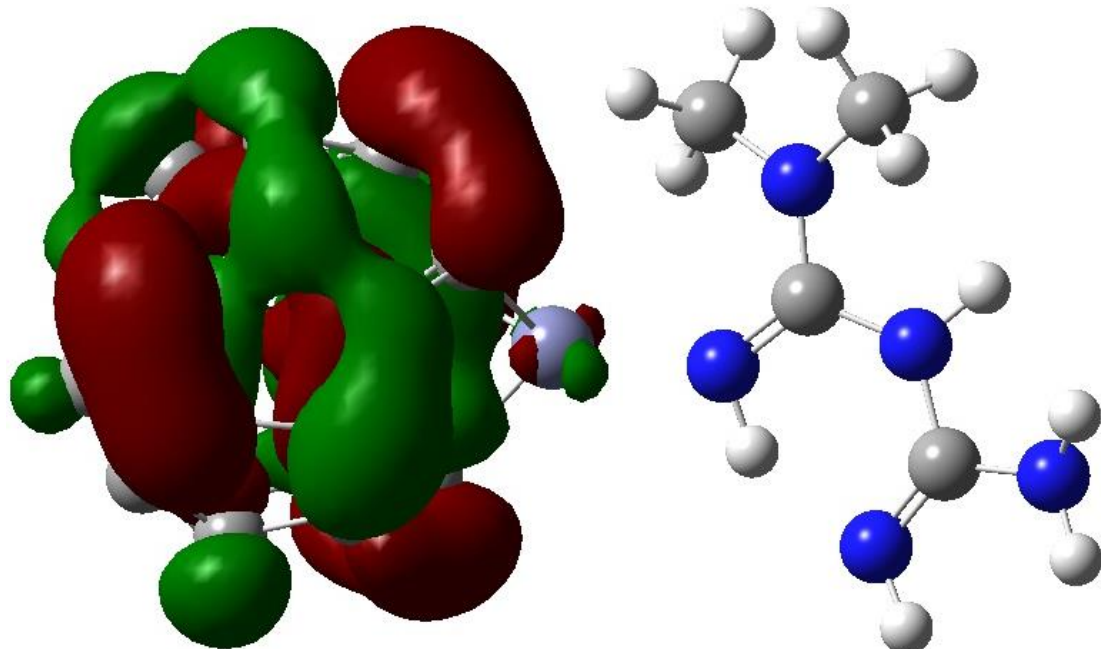


Figure 22. LUMO orbital of Solvent C23Zn M3

Gap Energy Calculation Review

To evaluate the electronic properties and stability of the metformin–fullerene complexes, the energy gap (E_{gap}) between the HOMO and LUMO orbitals was calculated for Fe-, Sc-, and Zn-doped C23

fullerene in the solvent phase (water). A smaller HOMO–LUMO gap typically indicates higher chemical reactivity, while a larger gap corresponds to increased stability of the electronic structure.

The results of the gap energy calculations are summarized in **Table 13**.

Table 13. HOMO, LUMO, and Energy Gap (E_{gap}) for Solvent-Phase C23 Fullerene Complexes

Sample	HOMO (eV)	LUMO (eV)	E_{gap} (eV)
Solvent C23Fe	-0.25130	-0.05569	5.3228
Solvent C23Fe-M2	-0.24869	-0.05074	5.3864
Solvent C23Fe-M3	-0.24621	-0.04933	5.3573
Solvent C23Sc	-0.23348	-0.02610	5.6430
Solvent C23Sc-M2	-0.23386	-0.02317	5.7331
Solvent C23Sc-M3	-0.22607	-0.01720	5.6836
Solvent C23Zn	-0.25555	-0.06823	5.0972
Solvent C23Zn-M2	-0.25201	-0.06504	5.0877
Solvent C23Zn-M3	-0.24900	-0.06302	5.0607

As shown in **Table 13**, all systems exhibit energy gaps in the range of **approximately 5.06–5.73 eV**, indicating relatively stable electronic structures in aqueous solvent. Sc-doped fullerene complexes (especially **Solvent C23Sc-M2**) show the **largest energy gaps**, suggesting the highest chemical stability. In contrast, Zn-doped systems exhibit slightly smaller gaps, indicating marginally higher reactivity. Metformin adsorption causes observable but moderate shifts in both HOMO and LUMO energies across all dopant types.

Load Analysis Review

Load Analysis Images

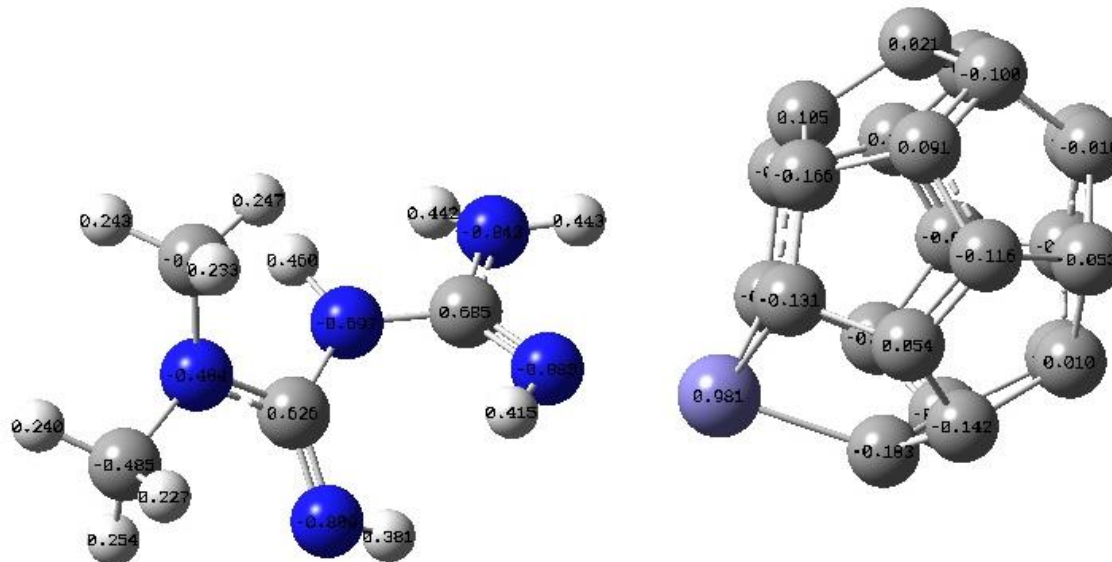


Figure 23. Load Analysis Solvent C23Fe M2

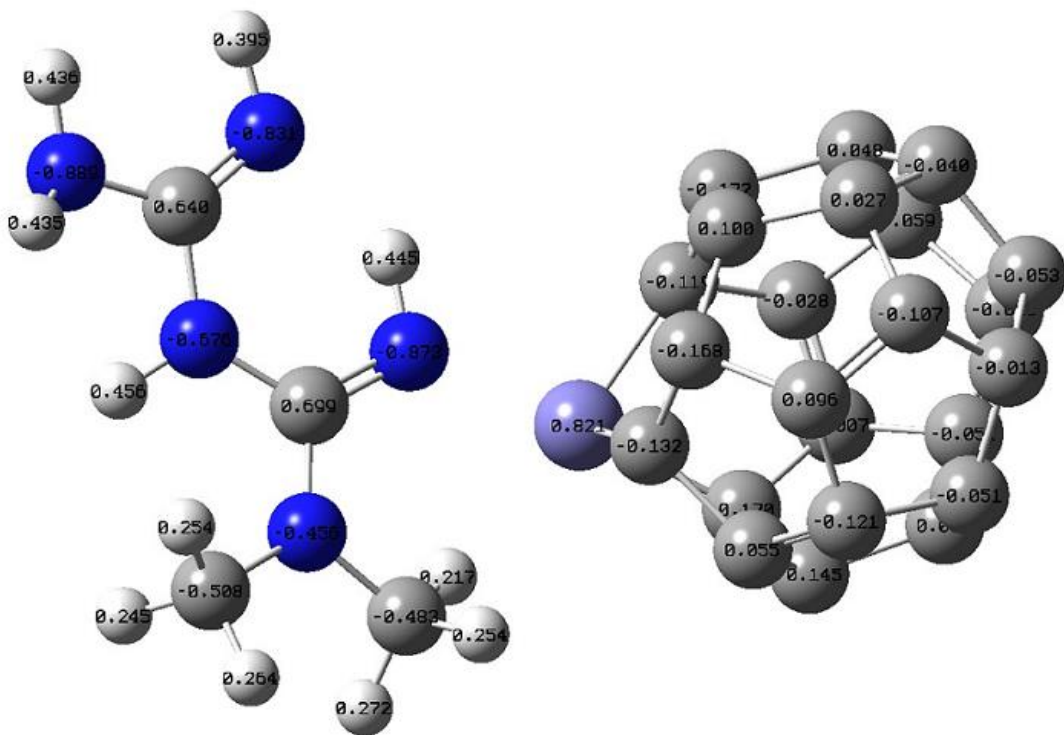


Figure 24. Load Analysis Solvent C23Fe M3

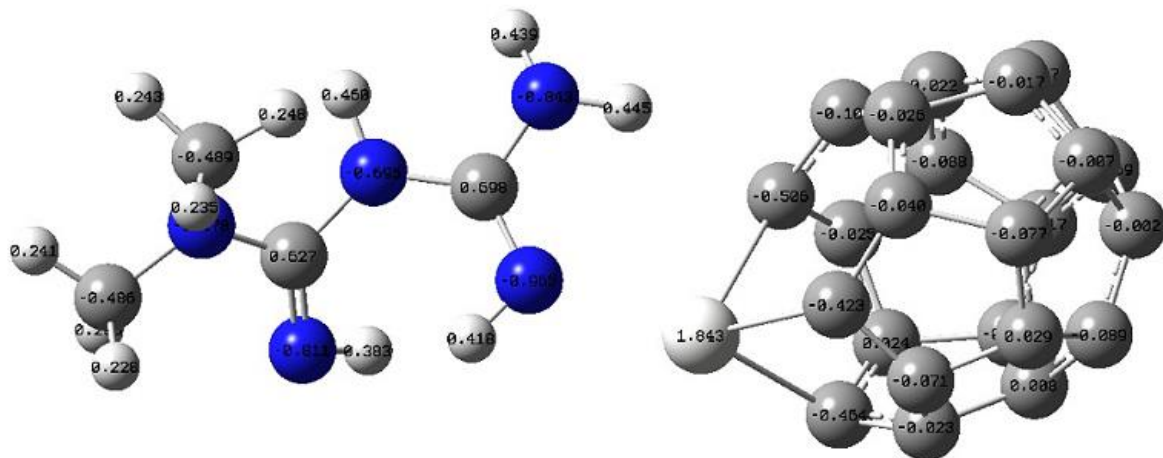


Figure 25. Load Analysis C23Sc M2 Solvent

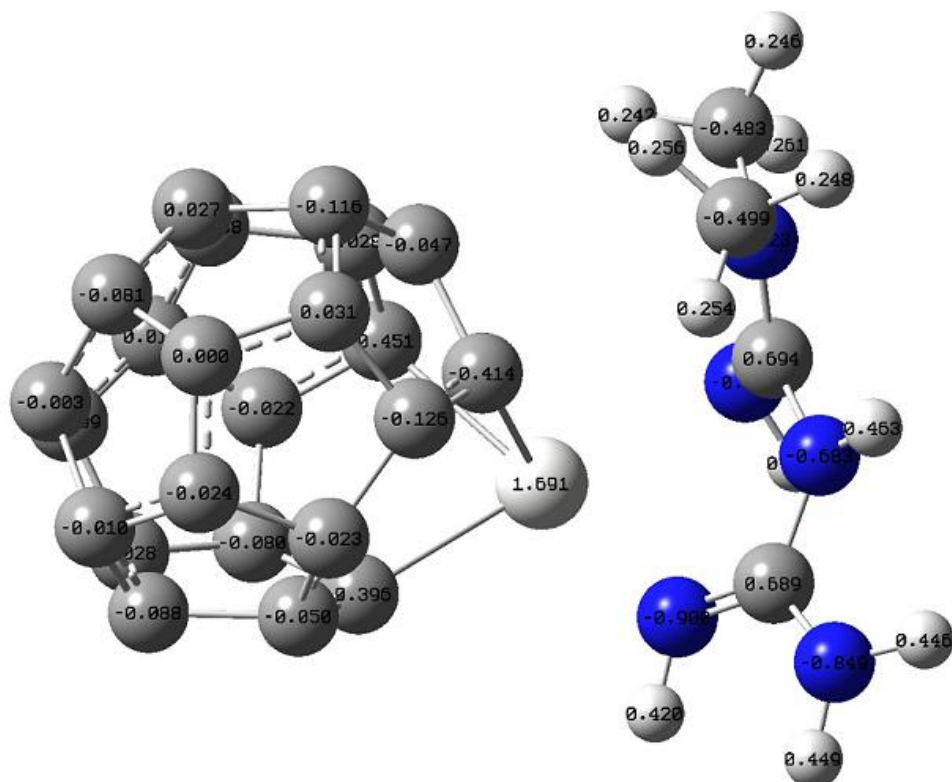


Figure 26. Load Analysis C23Sc M3 Solvent

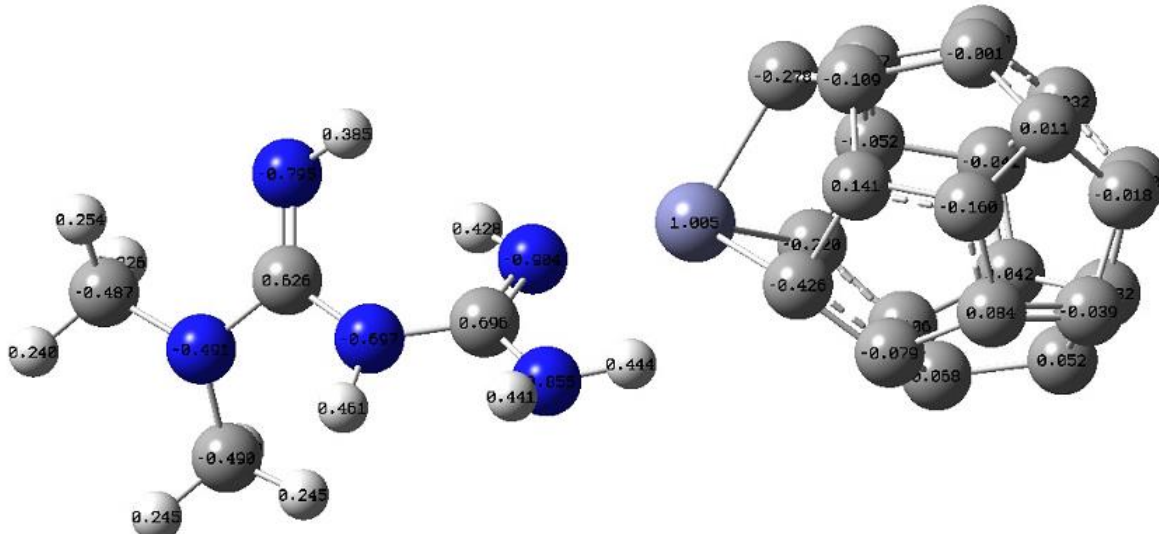
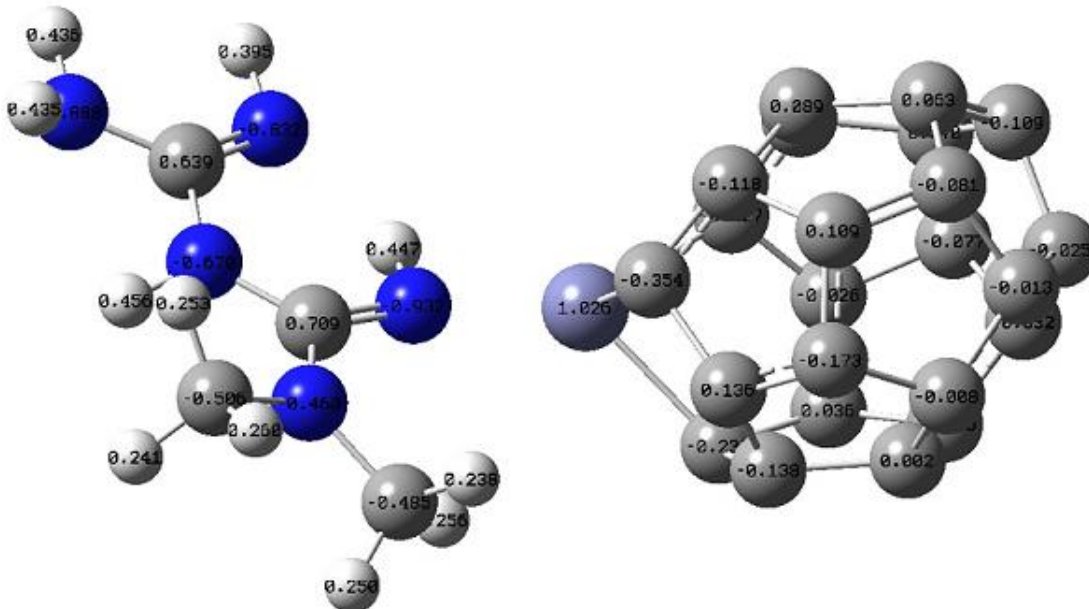


Figure 27. Load Analysis Solvent C23Zn M2

**Figure 28.** Load Analysis Solvent C23Zn M3

Load Analysis Calculation

To investigate the charge transfer behavior between metformin and the metal-doped fullerene complexes, load analysis (Q) was performed for each optimized structure in the solvent phase (water). This analysis helps determine how electron density is redistributed during adsorption, which is directly related to adsorption strength, reactivity, and stability.

The calculated load analysis values for Fe-, Sc-, and Zn-doped C23 fullerene systems are summarized in [Table 14](#).

Table 14. Load Analysis (Q) for Metformin Complexes with Fe-, Sc-, and Zn-Doped C23 Fullerene (Solvent Phase)

Sample	Load Analysis (Q)
Solvent C23Fe-M2	0.208
Solvent C23Fe-M3	0.296
Solvent C23Sc-M2	0.153
Solvent C23Sc-M3	0.304
Solvent C23Zn-M2	0.285
Solvent C23Zn-M3	0.234

As shown in [Table 14](#), all complexes exhibit positive load analysis values, indicating charge transfer from metformin toward the doped fullerene surface. The highest charge transfer occurs in **Solvent C23Sc-M3**, followed by **Solvent C23Fe-M3**, suggesting stronger electronic interaction and potentially enhanced adsorption stability for these configurations.

Discussion

In this study, we modeled and optimized the structure of C24 fullerene and its metal-doped derivatives, and systematically investigated the quantum chemical properties of the resulting complexes, including molecular structure, electronic stability, and reactivity parameters such as the energies of the highest occupied molecular orbital (HOMO) and the lowest unoccupied molecular orbital (LUMO), using **density functional theory (DFT)**. Adsorption energies and thermodynamic parameters, including Gibbs free energy (ΔG), enthalpy (ΔH), and entropy (ΔS), were calculated to evaluate the interaction of metformin with Fe-, Sc-, and Zn-doped fullerene adsorbents.

Enthalpy calculations were used to determine whether adsorption is exothermic or endothermic, while Gibbs free energy provided insight into the spontaneity of the adsorption process. The adsorption behavior of metformin was evaluated in different orientations on the doped fullerene surfaces. Results show that the adsorption energy strongly depends on both the orientation of the metformin molecule and the type of doped fullerene.

Chemical adsorption is characterized by strong intermolecular interactions and changes in electron density distribution between the adsorbate and the surface, typically accompanied by significant energy release compared to physical adsorption. Based on the adsorption energy values calculated for the different sites, it can be concluded that metformin adsorption on Fe-, Sc-, and Zn-doped fullerene is **chemically driven**, indicating strong interactions between metformin and the doped fullerene surfaces.

The calculated adsorption energies are summarized as follows:

- **C23Fe complexes:** M2 = -5471.35 kcal/mol, M3 = -4171.37 kcal/mol
- **C23Sc complexes:** M2 = -3324.27 kcal/mol, M3 = -4899.37 kcal/mol
- **C23Zn complexes:** M2 = -5617.33 kcal/mol, M3 = -3087.35 kcal/mol

Among these, the **C23Sc-M3 complex** exhibits the most favorable adsorption energy (-4899.37 kcal/mol) in solution, indicating the strongest interaction between metformin and the fullerene in this configuration.

Enthalpy calculations (Table 10) indicate **negative ΔH values** for all complexes, confirming that the adsorption process is exothermic. The C23Fe-M3 complex exhibits the largest enthalpy release, whereas C23Sc-M2 exhibits the smallest. Entropy analysis (Table 11) shows that the **C23Zn-M2 complex** has the highest molecular disorder upon adsorption, while the **C23Fe-M2 complex** is the most ordered. The combination of negative ΔH and ΔS values suggests that the adsorption of metformin on the doped fullerenes is **spontaneous at low temperatures**.

Gibbs free energy calculations (Table 12) further support this conclusion. The **C23Fe-M3 complex** exhibits the highest ΔG value, while **C23Sc-M2** shows the lowest. These results indicate that adsorption is generally spontaneous, with certain configurations being thermodynamically more favorable than others.

Electronic structure analysis (Table 13) reveals that the HOMO-LUMO gap (E_{gap}) of the isolated fullerenes is 5.32 eV for C23Fe, 5.64 eV for C23Sc, and 5.09 eV for C23Zn. Upon adsorption of metformin, the energy gaps of the complexes slightly increase (e.g., C23Fe-M2: 5.38 eV, C23Sc-M2: 5.73 eV), suggesting enhanced electronic stability and better adsorption performance relative to the pristine fullerenes.

Load analysis (Table 14) indicates that electron transfer occurs between the adsorbate and the fullerene surface. For example, metformin in **C23Zn-M2** donates electrons to the adsorbent, while in C23Fe-M2, C23Fe-M3, C23Sc-M2, C23Sc-M3, and C23Zn-M3, electrons are transferred from the fullerene to metformin. This charge redistribution contributes to the stability and chemical nature of adsorption.

Overall, the combined analysis of adsorption energies, thermodynamic parameters, electronic properties, and load transfer indicates that **metformin adsorption is most favorable on the C23Sc-M3 fullerene**, with an exothermic, spontaneous, and chemically driven adsorption process.

Recommendations and Future Work

- Investigate the effect of doping with other metals, including transition and noble metals, on adsorption performance.
- Perform adsorption studies using alternative DFT functionals and larger basis sets, such as **6-311++G(d,p)**, to improve accuracy.
- Study the effects of temperature and different solvent environments on the stability of the complexes.
- Explore doping with heavier metals, such as **gold or platinum**, to evaluate their potential for enhanced adsorption and catalytic activity.

References

Bibi, S., Ur-Rehman, S., Khalid, L., Bhatti, I. A., Bhatti, H. N., Iqbal, J., Bai, F. Q., & Zhang, H.-X. (2022). Investigation of the adsorption properties of gemcitabine anticancer drug with metal-doped boron nitride fullerenes as a drug-delivery carrier: a DFT study. *RSC Advances*, 12(5), 2873–2887. [Google Scholar] [Publisher] <https://doi.org/10.1039/D1RA09319C>

Esrafilii, M. D., & Khan, A. A. (2022). Alkali metal decorated C₆₀ fullerenes as promising materials for delivery of the 5-fluorouracil anticancer drug: a DFT approach. *RSC Advances*, 12(8), 3948–3956. [Google Scholar] [Publisher] <https://doi.org/10.1039/D1RA09153K>

Fekri, M. H., Bazvand, R., Soleymani, M., & Razavi Mehr, M. (2024). Adsorption of metronidazole drug on the surface of nano fullerene C₆₀ doped with Si, B and Al: A DFT study. *International Journal of Nano Dimension*, 11(4). [Google Scholar] [Publisher] <https://doi.org/10.57647/>

İskender Muz, * (2025). Fluoroquinolone antibiotic adsorption on the functional C₇₀ fullerenes: A computational insight on adsorbent applications. *Bitlis Eren Üniversitesi Fen Bilimleri Dergisi*, 14(1), 385–397. [Google Scholar] [Publisher] <https://doi.org/10.17798/bitlisfen.1592320>

Moumivand, A., Naderi, F., Moradi, O., & Makiabadi, B. (2025). Smart drug delivery: a DFT study of C₂₄ fullerene and doped analogs for pyrazinamide. *Nanoscale Advances*, 7, 1287–1299. [Google Scholar] [Publisher] <https://doi.org/10.1039/D4NA00560K>

Lin, B., Dong, H., Du, C., Hou, T., Lin, H., & Li, Y. (2023). Pristine B₄₀ fullerene as a potential gemcitabine drug carrier for anti-lung cancer properties: a DFT and QTAIM study. *Journal of Molecular Modeling*. [Google Scholar] [Publisher] <https://pubmed.ncbi.nlm.nih.gov/39578981/>

Sadeghzadeh, A., Sheikhshoiae, I., & Behpour, M. (2018). Adsorption of Celecoxib on B₁₂N₁₂ fullerene: Spectroscopic and DFT/TD-DFT study. *Journal of Physical Chemistry A*, 122(9), 2288–2295. [Google Scholar] [Publisher] <https://doi.org/10.1021/acs.jpca.7b11621>

Saha, S., & Pati, S. K. (2025). Metal-doped fullerene: promising electrocatalysts for hydrogen and oxygen evolution reactions. *Physical Chemistry Chemical Physics*, 27, 12024–12031. [Google Scholar] [Publisher] <https://doi.org/10.1039/D5CP01310K>